



ORIGINAL ARTICLE

Assessment of thermal stress risk in mass concrete elements: use of expedited diagrams

Avaliação do risco termo-tensional em elementos de concreto massa: uso de diagramas expeditos

Bruno Pessoa^{a,b} Carlos Brites^{a,c} Sérgio Botassi^d Jéssica Dantas^{c,e} Mariana Carvalho^f Douglas Couto^b Carlos Marmorato Gomes^b ^aBrites Consultoria, São Paulo, SP, Brasil^bUniversidade Estadual de Campinas – UNICAMP, Campinas, SP, Brasil^cUniversidade de São Paulo – USP, São Paulo, SP, Brasil^dSBS Consultoria, São Paulo, SP, Brasil^eCyrela, São Paulo, SP, Brasil^fInterCement Brasil, São Paulo, SP, Brasil

Received 07 September 2023

Revised 28 March 2024

Accepted 01 April 2024

Abstract: Large structural elements have been commonly observed in increasingly tall buildings, employing mass concrete elements in their foundations. In these elements, the internal heat generated by the cement hydration can be decisive for the occurrence of pathological manifestations arising from the balance of stresses and also by delayed ettringite formation. This article presents a practical and expedited method, through diagrams, for a preliminary assessment of the thermo-tensional risk involved in the concreting of large-scale elements. For the development of thermal risk diagrams, the commercial software TSA-2D was used, where 64 numerical computational simulations were conducted, varying the parameters with the greatest influence on the concrete thermal phenomenon (minimum dimension of the structural element, cement content per cubic meter, cement hydration heat, concrete placement temperature, and ambient temperature). The result of this methodology, when compared to computational simulations and field monitoring in a specific case study, showed a good correlation, with the potential for application and reproducibility, considering the natural limitations of an expeditious practice that needs to be evaluated on a case-by-case basis, but which provide an important guideline in the early decision-making on-site. Furthermore, the maximum absolute error between the results of computational simulation and field monitoring was only 1.6%.

Keywords: basement, mass concrete, concrete with ice, thermal simulations, thermal risk, cracking.

Resumo: Elementos estruturais de grande porte têm sido comum na implantação de edifícios cada vez mais altos, tendo em sua execução o concreto massa na solução da fundação. Nestes elementos, o acúmulo de calor interno gerado pela hidratação do cimento pode ser determinante para a ocorrência de manifestações patológicas, oriundas do equilíbrio de tensões e, também, pela formação de etringita tardia. Este artigo apresenta um método prático e expedito, por meio de diagramas, para avaliação preliminar do risco termo-tensional envolvido na concretagem de elementos de grandes proporções. Para o desenvolvimento dos diagramas de risco térmico utilizou-se o software comercial TSA-2D, onde foram realizadas 64 simulações numéricas computacionais variando os parâmetros com maior influência no fenômeno térmico do concreto (menor dimensão do elemento estrutural, consumo de cimento por metro cúbico, calor de hidratação do

Corresponding author: Bruno Pessoa. E-mail: brunopessoa.brites@gmail.com

Financial support: None.

Conflict of interest: Nothing to declare.

Data Availability: The data that support the findings of this study are available from the corresponding author, BP, upon reasonable request.



This is an Open Access article distributed under the terms of the Creative Commons Attribution License, which permits unrestricted use, distribution, and reproduction in any medium, provided the original work is properly cited.

cimento, temperatura de lançamento do concreto e temperatura ambiente). O resultado desta metodologia, ao ser comparado com simulações computacionais e monitoramento em campo em um estudo de caso específico, demonstrou boa correlação, com potencial de aplicação e reprodutibilidade, ponderando-se as naturais limitações de uma prática expedita que precisam ser avaliadas caso a caso, mas que garantem uma importante diretriz nas primeiras tomadas de decisão em obra. Além disso, o erro máximo absoluto entre os resultados da simulação computacional e monitoramento em campo foi de apenas 1,6%.

Palavras-chave: fundações, concreto massa, concreto com gelo, simulações térmicas, risco térmico, fissuração.

How to cite: B. Pessoa, C. Britez, S. Botassi, J. Dantas, M. Carvalho, D. Couto, C. M. Gomes, "Evaluation of thermal risk in mass concrete elements: use of expedited diagrams" *Rev. IBRACON Estrut. Mater.*, vol. 17, no. 4, e17412, 2024, <https://doi.org/10.1590/S1983-41952024000400012>

1 INTRODUCTION

In Brazil, notably, several researchers have delved into the subject of mass concrete in recent years [1]–[5]. In large metropolises, land restriction in prime areas has led to the production of tall buildings in smaller spaces, which implies high loads on the foundation elements. As a result, to guarantee stability, the foundation elements became massive, requiring the use of concepts that were developed and improved for decades in concrete dams. Some of these concepts will be presented below.

1.1 Mass concrete

Compared to so-called "normal" or "conventional" concrete, mass concrete exhibits a peculiarity: it struggles to dissipate the heat generated by the exothermic chemical reactions of cement hydration. This phenomenon leads to greater dimensional variations in the concrete, which, if constrained internally or externally [6], induces stress development influenced by various factors such as the thermal and mechanical properties of the material, element geometry, and ambient conditions. If these stresses exceed the tensile strength of the concrete at a given moment, thermal cracking occurs, allowing the ingress of aggressive agents and potentially compromising the structure's integrity [7]. Generally, mass concrete can be qualitatively defined as any volume of concrete with dimensions significant enough to require measures for controlling internal heat generation and resulting volume variations, aimed at minimizing cracking [8]–[10]. Moreover, the current trend of producing thinner and more reactive cement (with higher levels of C3S and C3A) to meet industry demands for higher initial strength within tighter construction schedules may exacerbate this issue [8].

Another concern related to overheating in mass concrete structures is the possibility of cracking caused by a thermochemical reaction known as DEF (Delayed Ettringite Formation). It occurs when the primary ettringite (a compound formed between calcium sulfate and aluminate), crucial for developing concrete properties, becomes unstable at high temperatures, typically around 65-70°C [11]. This instability promotes sulfate enrichment in the cementitious matrix, which, over months or even years, can lead to the formation of new ettringite through an expansive reaction. Depending on the quantity and size of the crystals formed, the resulting stresses may exceed the concrete's resistance, resulting in widespread cracking [12]–[14].

1.2 Numerical modeling

Hardening concrete presents one of the most challenging tasks in structural material modeling, owing to its complex microstructure and the transformations it undergoes during cement hydration. In addition to chemical reactions associated with hydration, numerous physical phenomena occur, such as phase changes, and various fields interact with each other (thermal, hygro, mechanical, etc.), rendering the problem multifield and multiphysics [15], [16]. Consequently, two approaches are commonly adopted:

- Pure thermo-chemical and mechanical models: These models treat concrete as a continuous medium and neglect detailed analysis of physical processes related to phase transitions and chemical reactions during hardening. Thermal strain is linked to temperature variation and the coefficient of thermal expansion, which remains constant for sufficiently accurate predictions [17]. Numerous studies have compared model estimations with experimental measurements [18]–[21].
- Multiphase models: These models consider not only the solid phase but also the liquid and gaseous components filling the material's pores, based on Multiphase Porous Media Mechanics (MPMM). They provide a precise analysis of physical phenomena and the influence of the material's internal structure. Validation of such models can be found in Pesavento et al. [15].

These simulations offer an effective means of evaluating thermal risk in mass concrete elements. Discretized models allow for the analysis of two fundamental factors: temperature, ensuring it does not exceed 65°C/70°C internally, and stress, ensuring it does not surpass concrete tensile strength. However, the utilization of these analyses often requires specialized software and expertise, limiting their widespread application.

1.3 Research Significance

In practical terms, it sometimes occurs that due to a lack of appropriate knowledge and practical procedures to assist in defining structural elements requiring special attention regarding concrete's thermal issues, many concreting operations are still carried out without precaution or prudence to mitigate such problems.

In building construction, common doubts arise regarding which elements should be treated as mass concrete structures. Many available recommendations are based on a limited set of variables, often restricted to considerations related to volume, making them susceptible to inaccuracies.

In this context, this article presents a preliminary methodology tool for evaluating thermal-tensional risk using quick and comprehensive diagrams. The aim is to identify situations where additional control measures are necessary to minimize the effects of internal heat generation in mass concrete elements. The entry data for this tool include cement content, the heat of hydration, the smallest dimension of the element (height), concrete placement temperature, and ambient temperature. The authors did not find a similar proposal in the consulted literature, making this preliminary analysis methodology using expedited diagrams unprecedented. The tool is intended to guide and facilitate decision-making regarding thermo-tensional modeling, considering input parameters that are easily obtained from mass concrete works.

However, it is important to note that the use of this preliminary tool does not replace the analysis of stress balance, as it focuses solely on internal temperatures and their gradients. Extrapolation for stresses requires a more refined analysis using specific thermal simulation programs [6], [22]. Even though, in regions of low and moderate risk on the diagram, applied stresses tend to be potentially lower than the tensile strength, this does not exempt the need for complementary analysis through thermal simulation.

2 CONCEPTS OF THERMAL RISK

Determining thermal risk in mass concrete elements is complex due to the simultaneous action of several factors, making it challenging to generate models that accurately represent real conditions on-site [6], [22].

According to ACI 301-10 [23], if the minimum dimension of the concrete element exceeds 1.20 m and/or the cement consumption of the concrete mix surpasses 390 kg/m³, deleterious effects related to thermal issues may arise.

Vicente et al. [24], using computer simulations, demonstrated that foundation blocks composed of concrete with compressive strength (f_{ck}) \geq 40 MPa, cement consumption of 422 kg/m³, and plan dimensions equal to or greater than 3 m, with a height exceeding 1 m, may reach internal temperatures close to 65°C, indicating considerable susceptibility to thermal risk.

Demétrio et al. [25] suggest that elements with the smallest dimension greater than 60 cm should be treated as mass concrete elements.

Botassi [6] notes that concretes with compressive strength (f_{ck}) ranging from 45 to 90 MPa, cement consumption between 400 and 650 kg/m³, and the smallest dimension equal to or greater than 40 cm, may already require specific thermal assessment.

It is observed that the smallest dimension of the element is a commonly used parameter for estimating preliminary thermal risk in concrete structures. However, Bobko [26] reported significant divergence among recommended values by various international entities, ranging from 0.90 m to 1.80 m. Thus, making an assertive definition solely based on this criterion is challenging.

Another existing method, which considers only the geometry of the element, is the massivity index (M) proposed by ACI 207.2R [27] (Equation 1). This index represents the relationship between the volume and the exposed surface of the element, providing a comparative perception of thermal risk, with higher massivity indexes indicating greater risk.

$$M = \frac{\text{Volume}}{\text{Exposed surface}} \quad (1)$$

Where:

Exposed surface: the one in direct contact with the air.

Regrettably, there are no provided boundary values that would allow the classification of the structure as massive.

Concurrently, Botassi [6] presents an equation (Equation 2), valid for concretes made with cement CP I, CP II, and CP V according to ABNT NBR 16697 [28] and strength class up to C40, with low thermal risk when the result is equal to or less than 0.5, medium, when the result is between 0.5 and 0.8, imminent, when the result is between 0.8 and 1.4 and higher, when the result is greater than 1.4.

$$Thermal\ risk = \frac{Volume \times Smallest\ dimension}{Exposed\ surface} \quad (2)$$

Where:

Exposed surface: the one in direct contact with the air.

Another alternative approach to the concept of massivity, where the limits for classifying a structure as massive are also presented, is proposed by Flaga [29], who uses the concept of surface modulus (Equation 3).

$$M_S = \frac{Exposed\ Surface [m^2]}{Volume [m^3]} \quad (3)$$

For M_S values below 2, the structures are considered massive, with a predominant impact of thermal shrinkage and a condition close to the adiabatic state in their core. For M_S values between 2 and 15, the structures are classified as “semi-massive”, presenting a considerable impact from drying and thermal shrinkage. For M_S values above 15, the structures are classified as “thin walls”, with a negligible thermal impact.

It is noted that equations based on the principle of massivity, which exclusively takes into account the geometry of the element, provide a simple and relatively quick assessment of the potential for thermal cracking. However, the influence of several other factors, in addition to geometry, significantly affects the assessment of concrete's thermal risk, limiting the accuracy of these equations.

In this regard, recently, Kanavaris et al. [30] aimed to obtain more accurate estimates by proposing the improved massivity index (M_{cor}) (Equation 4) as an enhancement of the surface modulus (M_S). This modification incorporates dimensionless coefficients representing the effects of cement type, its content, and the temperature differential reached by the structure.

$$M_{cor} = \frac{M_S}{k_f \times k_b \times k_{\Delta T}} \quad (4)$$

Where:

k_f is a correction factor for the potential hydration heat released by a cement other than that considered in the standard mass index (Type I Cement according to ASTM C150/C150M [31]). This coefficient is calculated using the ratio between the heat of hydration of the cement to be used (Q_{scm} , in J/g) by the heat of cement type I (Q_{cemI} , in J/g) admitted equal to 366 J/g, according to Equation 5.

$$k_f = \frac{Q_{scm}}{Q_{cemI}} \quad (5)$$

k_b is the correction factor related to the cement content, calculated through Equation 6.

$$k_b = \frac{Cement\ content}{300} \quad (6)$$

$k_{\Delta T}$ is the correction factor related to the temperature differential, calculated through Equation 7.

$$k_{\Delta T} = \frac{T_{fresh} - T_{ambient} + T_{adi, rise}}{T_{adi, rise}} \quad (7)$$

Where:

T_{fresh} is the concrete placing temperature;

$T_{ambient}$ is the outside temperature;

$T_{adi,rise}$ is the internal temperature rise due to cement hydration under adiabatic temperature conditions, which may be estimated according to Figure 1.

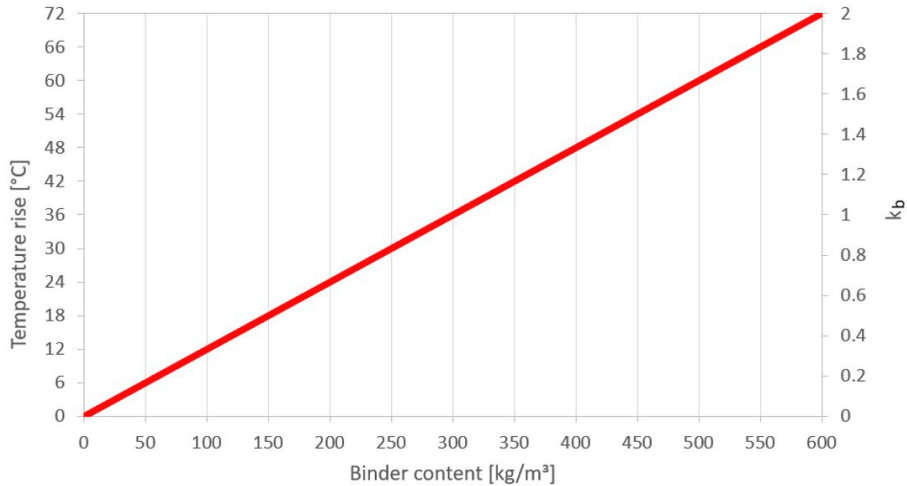


Figure 1. Relationship between binder content and approximated temperature rise in concrete and k_b correction factor [27].

This approach, when compared with the original massivity index, yields more reliable results [30]. However, it is important to highlight that this is a simplified method in which the constants of the enhancement coefficients were proposed through a practical approach. Furthermore, this method does not consider restriction levels, as well as the thermal and mechanical properties of concrete. Therefore, as concluded by the authors, further refinements and validations through computer simulations are necessary.

Concurrently, Gajda [32] presents the results of exhaustive computer simulations in the form of a graph (Figure 2) depicting the combination of cement content and the minimum dimension of the element. This graph forms a map with three levels of thermal risk based on these bi-univocal compositions. The green region indicates low thermal risk, the yellow region represents an indeterminate range subject to the user's discretion, and the red region signifies high thermal risk, suggesting that elements falling within this area must be treated as mass concrete.

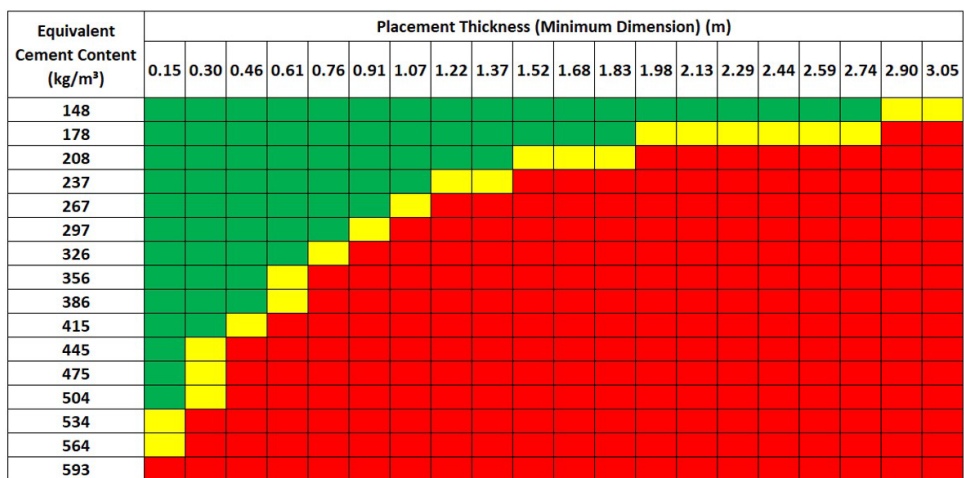


Figure 2. Minimum dimension x Equivalent cement content for normal density concrete (Adapted from Gajda [32]).

The proposed methodology stands out not only for its practicality compared to the application of massiveness coefficients but also for its expected ability to yield more accurate results. This is because the method was developed based on the outcomes of computational simulations, enhancing its accuracy. However, the main challenge lies in considering heat generation, where binder consumption and hydration heat are taken into account through an “equivalent content.” This equivalent content is calculated based on a series of weightings related to the number of additives of each type of cement, with the method initially developed for American type I and II types of cement according to ASTM C150/C150M [31]. This may pose a challenge in the Brazilian context, given the wide variation allowed in these additives during cement manufacturing. Additionally, the method does not address considerations related to concrete properties nor specify any potential restrictions for its application.

3 METHOD

To achieve greater accuracy in assessing potential thermal risks using quick diagrams, five parameters strongly influencing the thermal phenomenon in mass concrete were correlated. These parameters include the minimum dimension of the structural element (height), cement content per cubic meter, cement hydration heat, concrete placement temperature, and ambient temperature.

For the development of the thermal hazard diagrams, TSA 2D software, version 5.9 of 2021 [33], was utilized and compared with several case studies of real works, calculated through computer simulations. This software enables modeling in the thermo-chemical-mechanical field and simulation of mass concrete elements at early ages in a transient regime, using the finite element method (FEM) to resolve temperature and stress fields. Sixty-four computational numerical simulations were conducted (see Figure 3), divided into two sets of thirty-two simulations each.

The first set considered concrete casting in the formwork at a temperature of 20°C, taking into account the possibility of cooling the concrete. The second set of simulations considered concrete pouring at a temperature of 30°C. Each set of thirty-two simulations was further subdivided into sixteen simulations for each minimum dimension considered, namely 1 meter and 3.5 meters, respectively.

Within these sets, four simulations were conducted for each cement consumption rate, established at 300, 340, 380, and 420 kg/m³. The cement hydration heat at 168 hours was varied to predefined values of 250, 290, 320, and 360 J/g.

Confection of diagrams (64 simulations)			
Concrete placing temperature = 20 °C (32 simulations)		Concrete placing temperature = 30 °C (32 simulations)	
Minimum dimension = 1.0 meter (16 simulations)	Minimum dimension = 3.5 meters (16 simulations)	Minimum dimension = 1.0 meter (16 simulations)	Minimum dimension = 3.5 meters (16 simulations)
Cement content: 300 kg/m ³ H.H.: 250, 290, 320 and 360 J/g (4 simulations)	Cement content: 300 kg/m ³ H.H.: 250, 290, 320 and 360 J/g (4 simulations)	Cement content: 300 kg/m ³ H.H.: 250, 290, 320 and 360 J/g (4 simulations)	Cement content: 300 kg/m ³ H.H.: 250, 290, 320 and 360 J/g (4 simulations)
Cement content: 340 kg/m ³ H.H.: 250, 290, 320 and 360 J/g (4 simulations)	Cement content: 340 kg/m ³ H.H.: 250, 290, 320 and 360 J/g (4 simulations)	Cement content: 340 kg/m ³ H.H.: 250, 290, 320 and 360 J/g (4 simulations)	Cement content: 340 kg/m ³ H.H.: 250, 290, 320 and 360 J/g (4 simulations)
Cement content: 380 kg/m ³ H.H.: 250, 290, 320 and 360 J/g (4 simulations)	Cement content: 380 kg/m ³ H.H.: 250, 290, 320 and 360 J/g (4 simulations)	Cement content: 380 kg/m ³ H.H.: 250, 290, 320 and 360 J/g (4 simulations)	Cement content: 380 kg/m ³ H.H.: 250, 290, 320 and 360 J/g (4 simulations)
Cement content: 420 kg/m ³ H.H.: 250, 290, 320 and 360 J/g (4 simulations)	Cement content: 420 kg/m ³ H.H.: 250, 290, 320 and 360 J/g (4 simulations)	Cement content: 420 kg/m ³ H.H.: 250, 290, 320 and 360 J/g (4 simulations)	Cement content: 420 kg/m ³ H.H.: 250, 290, 320 and 360 J/g (4 simulations)

Figure 3. Methodology for the development of thermal risk diagrams. Note: H.H.: Heat of hydration at 168h measured using the Langavant bottle test (ABNT NBR 12006:1990) [34].

3.1 Limitations and restrictions

The expedited thermal risk analysis diagrams are applicable for concrete elements that have the following conditions:

- Compressive strength (axial) at 28 days (f_{ck}) ≥ 40 MPa;
- Modulus of elasticity at 30% breaking load ≤ 30 GPa at 28 days of age;
- Density between 2,200 and 2,500 kg/m³;
- Large structural elements, with emphasis on foundation blocks, footings, and rafts, whose minimum dimension is greater than 100 cm (1 m) and the others greater than 300 cm (3 m), and also with a contact area with the subgrade on its base and/or relevant sides (usually ground).

It is inferred from these conditions that other structural elements subject to thermal risk are not subject to the application of the diagrams, as in the case of columns and beams of large sections, special structural elements of dams, and bridge elements, among others.

3.2 Hypotheses assumed

Some hypotheses for using the expedited thermal risk assessment diagram were adopted conservatively and will be presented below.

3.2.1 Properties adopted for the supporting soil

To obtain a good correlation with reality, in computational simulation, the consideration of materials contiguous to the main material (concrete) is allowed. So, to represent the supporting soil, the properties shown in Table 1 were adopted.

Table 1. Properties adopted for the support soil.

Thermal Conductivity ⁽⁶⁾	Density ⁽³⁾⁽⁵⁾	Specific Heat ⁽²⁾⁽¹⁾	Thermal expansion ⁽⁵⁾	Modulus of elasticity ⁽⁴⁾⁽⁵⁾
(W/m.°C)	(kg/m ³)	(J/kg.°C)	(10 ⁻⁶ /°C)	(GPa)
0.694	1800	1000	2.00	0.002

Source: ⁽¹⁾Botassi [22]; ⁽²⁾Vicente et al. [24]; ⁽³⁾Botassi [35]; ⁽⁴⁾Emborg [36]; ⁽⁵⁾Kreith and Black [37]; ⁽⁶⁾Funahashi et al. [38]

3.2.2 Properties adopted for concrete

The thermal properties of concrete are strongly influenced by aggregates, especially the coarse ones. In the city of São Paulo, there is a predominance of limestone and granite lithology aggregates, therefore, the thermal properties of concrete were established based on these characteristics (Table 2).

Table 2. Properties adopted for concrete

Thermal Conductivity ⁽¹⁾	Density ⁽¹⁾	Specific Heat ⁽²⁾	Thermal expansion ⁽³⁾
(W/m.°C)	(kg/m ³)	(J/kg.°C)	(10 ⁻⁶ /°C)
2.669	2401.5	947	10.00

Source: ⁽¹⁾ACI 207.2R-07 [27]; ⁽²⁾Gamballe et al. [39]; ⁽³⁾ABNT NBR 6118 [40].

For the mechanical properties, a compressive strength of concrete at 28 days (f_{ck}) equal to 40MPa was considered, and its evolution with time (up to 28 days of age) was defined based on Equation 8 (item 12.3.3 of ABNT NBR 6118:2014 [40]) considering the type of cement as CP III and CP IV with $s=0.38$. The tensile strength ($f_{ct,m}$, Equation 9) and the modulus of elasticity of concrete (E_{ci} , Equation 10) were estimated from the compressive strength (Equation 8), also recommended by the same Brazilian standard, addressed in items 8.2.5 and 8.2.8, respectively.

$$f_{ck,j} = e^{(0.38 \times \left[1 - \left(\frac{28}{t}\right)^{\frac{1}{2}}\right])} \times f_{ck} \quad (8)$$

$$f_{ct,m,j} = 0.3 \times (f_{ck,j})^{2/3} \tag{9}$$

$$E_{ci,j} = 0.9 \times 5600 \times (f_{ck,j})^{1/2} \tag{10}$$

The viscoelasticity of the material was considered through the creep function of the Bureau of Reclamation [41]. The coefficients of this function were obtained using the expression by Botassi et al. [42].

3.2.3 Temperature elevation

The temperature increase resulting from exothermic cement hydration reactions primarily depends on the heat release rate of the cement, which is an intrinsic property of the material, as well as its content per cubic meter. The heat release rate of a specific cement can be measured using standardized tests, such as the method outlined in ABNT NBR 12006:1990 [34], commonly utilized by cement and concrete companies.

Figure 4 shows the hydration heat curves of the main cement available in the city of São Paulo, measured by the Langavant Bottle method [34]. In the simulations, to build the diagrams, hydration heat curves were parameterized through the final value of 168 h, whose evolution over time was defined as a function of the average of the four curves.

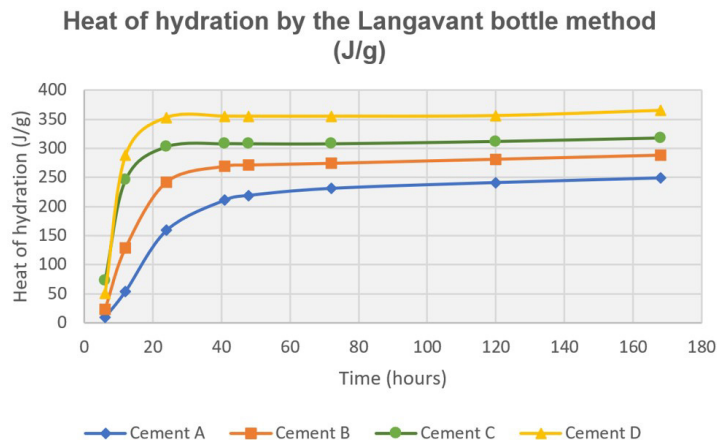


Figure 4. The heat of hydration of the main cement available in the city of São Paulo. Note: This figure was prepared based on the results of the heat of hydration tests of the four main types of cement that serve the São Paulo market, de from technical consultancy services that the authors provided between 2021 and 2022.

3.2.4 Boundary conditions and dimensions of the “standard” computational model

The dimensions of the computational model in plan view were defined as 10 m x 10 m with heights of 1 m and 3.5 m. The ambient temperature considered was 25°C (close to the annual average of São Paulo). Heat exchange by convection was estimated at the top of the structural element (13.5 W/m²/°C) and at the sides (3.0 W/m²/°C) [43], with heat exchange between concrete/air (without curing damp) and concrete/wooden formwork, respectively.

3.2.5 Cracking risk

The thermal cracking risk analysis used in the diagrams assumes that when the internal tensile stresses induced by thermal effects exceed the mechanical resistance, represented by the tensile strength, there is a likelihood of concrete cracking. This concept has been discussed extensively in the works of Botassi [6], [22], as well as in other reputable sources [7], [8], and [10].

The thermo-tensional analysis employed in the TSA-2D software, used for developing the diagrams, utilizes a thermo-coupled viscoelastic model. This means that stresses are calculated in the elastoplastic state of concrete, considering the effects of creep, and concrete properties are influenced by the temperature generated by the hydration reaction of the binders, based on the maturity model of the Arrhenius function.

A post-cracking structural damage analysis model was not included in the diagram development, as the onset of cracks is typically considered detrimental to structures subject to thermal effects, reaching the ELS (Elastic Limit State) and, in more critical situations, the ELU (Ultimate Limit State) [6].

4 RESULTS, DISCUSSION AND CASE STUDY

Figures 5 and 6 present the expedited diagrams of thermal risk under two conditions: with the concrete pouring temperature at 30°C (probably without ice) (Figure 5) and 20°C, probably with ice (Figure 6), with an ambient temperature of 25°C, close to the annual average for São Paulo.

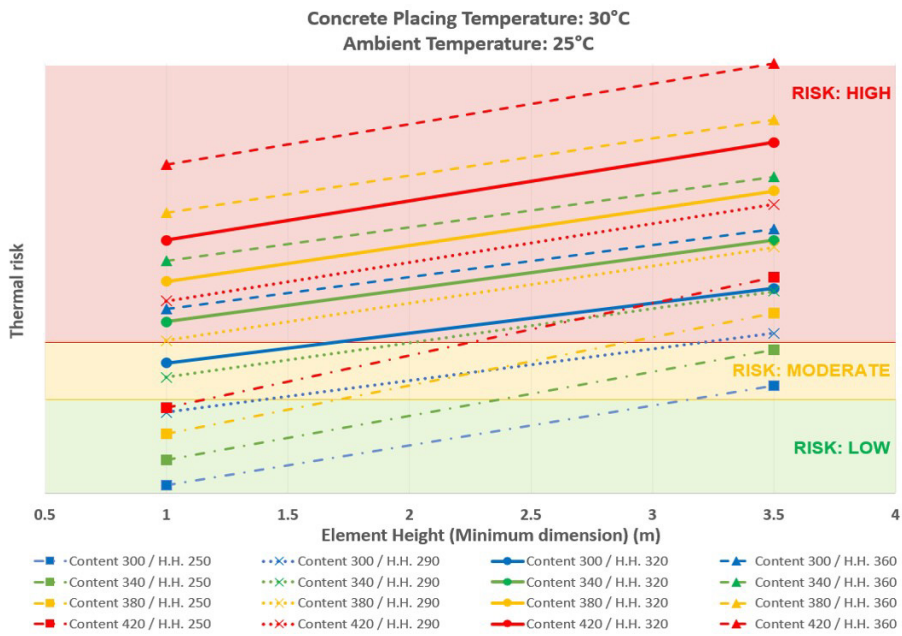


Figure 5. Diagram of thermal risk (Concrete Placing Temperature = 30°C)

Note: H.H. = Heat of hydration in Joule/gram at 168h, measured using the Langavant bottle test (ABNT NBR 12006:1990) / Content = Cement content of the concrete mix in kg/m³.

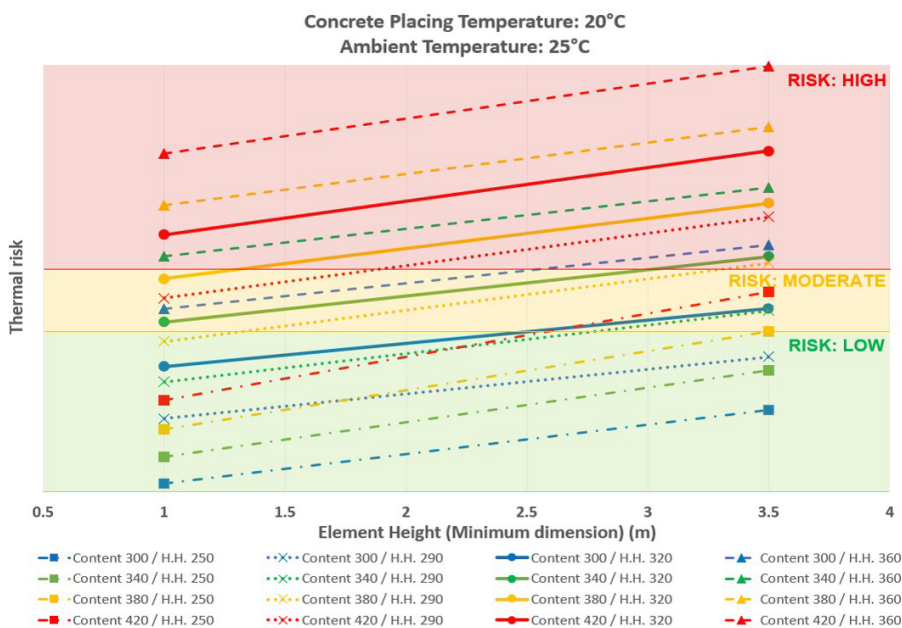


Figure 6. Diagram of thermal risk (Concrete Placing Temperature = 20°C)

Note: H.H. = Heat of hydration in Joule/gram at 168h, measured using the Langavant bottle test (ABNT NBR 12006:1990) / Content = Cement content of the concrete mix in kg/m³.

The thermal risk limits were determined based on technical literature, considering the maximum temperature peak in the structure and indirectly the potential tensional effects leading to cracking, aiming to simplify the modeling process. To utilize the diagrams, three measures must be known (assuming the ambient temperature and concrete placing temperature are fixed): the height of the structural element (starting from 100 cm), hydration heat at 168h, and cement content in the suggested combinations presented, which allow for interpolation in more specific cases. By selecting the most suitable combination (indicated by the sloping lines displayed in the graph area), one can parameterize with the minimum dimension of the element on the abscissa axis and, thus, determine the thermal risk in the graph region along the ordinate axis, indicated both by name and colorimetric indicator.

As mentioned by Mehta and Monteiro [8], more reactive cement is appreciated by the industry because it develops initial strengths more rapidly, allowing faster formwork removal. On the other hand, they tend to release greater amounts of heat, which can be a problem for mass concrete structures. In this context, it is highlighted in Figure 6 that there is a possibility that a concrete mix, with the same cement content, could incur in three different thermal risks (low, moderate, and high), when considered to compose an element whose minimum dimension is 1 meter. This distinction will depend on the reactivity of the cement, measured by its heat of hydration, most notably the value in Joules/gram of cement at 168 h.

It is also noted in Figures 5 and 6 that for the same hydration heat curve, the slope of the lines (inclination) remained practically unchanged. However, the slope was higher for cement with lower hydration heat. Precisely, the lines with a higher slope, or greater increase in thermal risk with the increase in height, occurred for the cement with 250 J/g at 168 hours.

This phenomenon can be attributed to the slower release of heat in the initial phases, causing a delay in the internal temperature peak. This condition facilitates greater heat exchange with the environment in blocks of lesser height, resulting in a lower relative internal temperature, while in taller blocks this exchange becomes progressively more difficult.

Taking as an example the comparison between the lines Content 380 / H.H. 250 and Content 300 / H.H. 290, the former would have a heat release about 10% higher than the latter, under adiabatic conditions. However, its thermal risk, associated with lower internal temperatures, proved to be lower at a height of 1 meter, whereas at a height of 3.5 meters, this condition was reversed.

4.1 Case study

A case study is presented below, of a work whose structural element object of analysis is a foundation block with plan dimensions of 12.65 m and 8.5 m with a height of 2.7 m, resulting in a volume of approximately 290 m³. Initially, a qualitative assessment was conducted using diagrams to evaluate the thermal risk associated with the pouring process. Subsequently, computer simulations were performed using TSA-2D software (version 5.9, 2021) to assess the accuracy of the responses obtained from the diagrams. Additionally, the foundation block was instrumented with thermocouples connected to data loggers to measure the internal temperature rise, particularly at the geometric center of the block, with temperatures recorded hourly.

Design requirements were f_{ck} of 40 MPa and E_{cs} ($0.3 f_c$) of 30 GPa at 28 days of age. Table 3 shows the concrete mix used.

Table 3. Concrete mix design applied in the structure.

Cement CPIII 40-RS ⁽¹⁾	Silica fume	Natural Sand	Artificial Sand	Gravel 9,5mm	Gravel 19mm	Admixture	Water + Ice
(kg/m ³)	(kg/m ³)	(kg/m ³)	(kg/m ³)	(kg/m ³)	(kg/m ³)	(kg/m ³)	(L/m ³)
342	22	332	498	212	847	3.0	182

Note: ⁽¹⁾According to ABNT NBR 16698:2018 [28].

The heat of hydration of the cement used in the mix design (Table 3) was characterized, and the values are shown in Table 4.

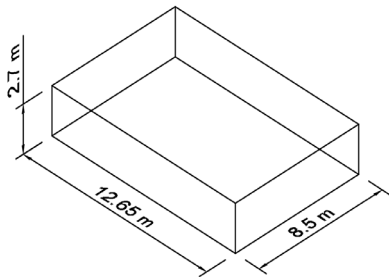
Table 4. Heat of hydration curve for the cement considered in the mix design.

Heat of hydration by the Langavant bottle method (J/g) (ABNT NBR 12006:1990)							
6 hours	12 hours	24 hours	41 hours	48 hours	72 hours	120 hours	168 hours
23	129	242	269	271	274	281	288

The input parameters needed for the thermal risk analysis through diagrams assessment are shown in Table 5.

Table 5. Volumetric representation and input parameters for consulting the thermal risk diagram.

Input parameters	Values	Measurement units
Minimum dimension (height)	2.70	meters
Cement content	342	kg/m ³
Cement hydration heat	288	J/g (168h)
Placing temperature	≤ 30	°C
Average ambient temperature	25	°C



With the initial data, the diagram can be consulted (Figure 7), following the steps:

1. On the abscissa axis (X axis), draw a vertical line at the coordinate next to 2.7 m, referring to the minimum dimension of the element under study (height) (indicated with the number 1, in Figure 7);
2. The second straight line will be drawn based on the heat of hydration and cement consumption data. To do this, choose the most convenient position on the diagram for the inclined **Cement content 342 / H.H. 288**, already located in Figure 7 (indicated with the number 2);
3. The thermal risk level is then obtained at the intersection of lines 1 and 2, and as a result, we have a high risk, indicating that, if produced as shown, cracking due to thermal problems would be a very likely consequence (High Risk).

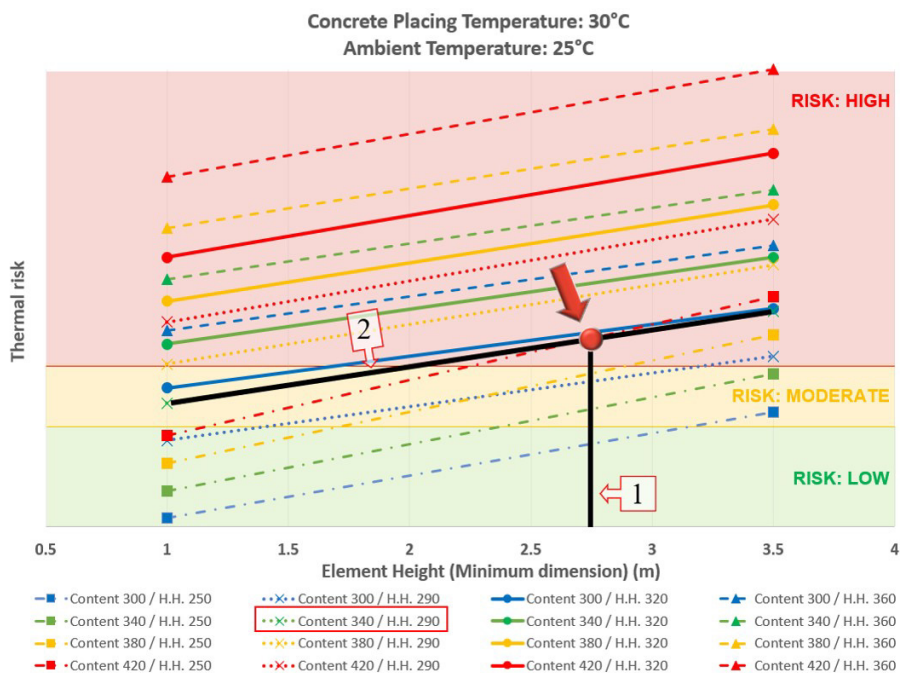


Figure 7. Evaluation of the risk of thermal cracking for cement content 342 / C.H. 288. Note: H.H. = Heat of hydration in Joule/gram at 168h, measured using the Langavant bottle test (ABNT NBR 12006:1990) / Content = Cement content of the concrete mix in kg/m³.

The response provided by the diagram indicates the necessity for additional measures to address the thermal issue. Some possible recommendations include: conducting a rational dosage study aimed at reducing cement consumption

(which has already been carried out in the laboratory phase, including the replacement of part of the cement with pozzolanic additions such as silica fume), replacing the current cement with one that has a lower hydration heat (also explored during the laboratory phase), dividing the element into layers during concreting, pre or post-cooling of the concrete, among others. These options require further investigation for a comprehensive assessment of the problem and for proposing the most suitable solutions.

In the following (Figure 8), the level of thermal risk associated with pouring the same structural element is assessed, this time considering the casting of concrete in forms at temperatures equal to or lower than 20°C (as depicted in the diagram in Figure 6). It is evident that, for this purpose, in the city of São Paulo, it is necessary to cool the concrete, for example, by replacing a portion of the mixing water with ice.

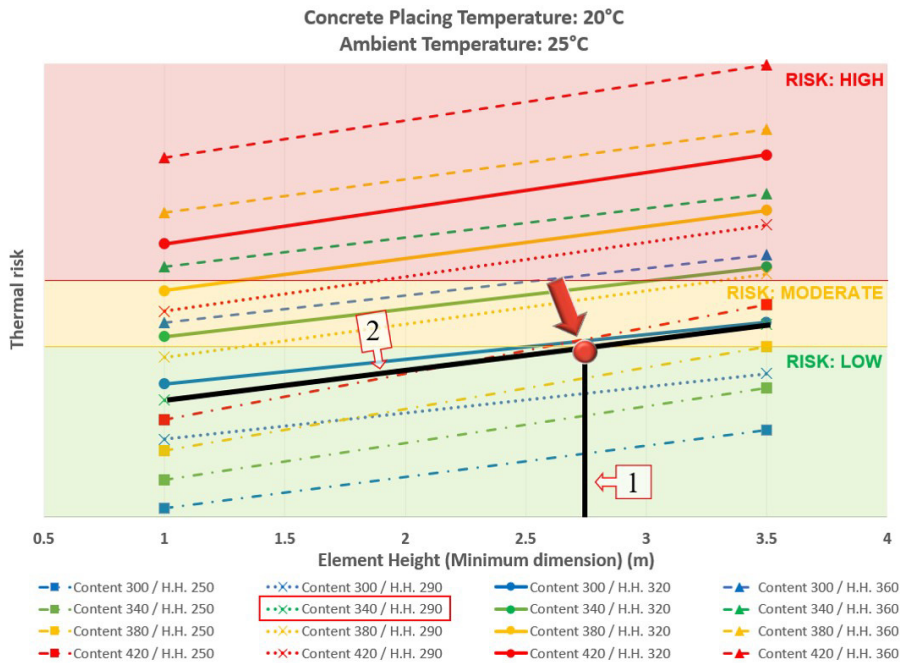


Figure 8. Evaluation of the risk of thermal cracking for cement content 342 / C.H. 288. Note: H.H. = Heat of hydration in Joule/gram at 168h, measured using the Langavant bottle test (ABNT NBR 12006:1990) / Content = Cement content of the concrete mix in kg/m³.

This time, the analysis indicates a low risk of thermal cracking. Therefore, it is understood that if implemented under these conditions, temperatures would likely not exceed 65°C.

4.2 Validation: computational thermomechanical simulations

As previously mentioned, in the computational simulations that generated the thermal risk diagrams, and to broaden their applicability, average thermal properties typical of concretes produced with granitic and limestone aggregates were considered due to their greater availability in the city of São Paulo. However, for the upcoming case study involving a real construction project, the simulations were conducted using the specific concrete mix of the project, with thermal properties characteristic of concretes primarily made from limestone aggregate lithologies (as detailed in Table 6). It is important to highlight that, as the diagrams aim to provide a qualitative response in terms of risk, these slight modifications in the thermal properties did not show a significant impact on the results.

For direct comparison with the diagrams, concrete placing temperatures of 30°C and 20°C will be considered, with the potential use of ice. Table 6 summarizes the data adopted for the computational thermomechanical study. The TSA-2D software (version 5.9, 2021) was utilized for the thermomechanical simulations, employing a square-type mesh with a maximum dimension of 25 cm, as depicted in Figure 9c.

Table 6. Summary of data adopted for the computational thermomechanical study.

Property	Description	Material	
		Concrete	Support soil
Physical	Density (kg/m ³)	2446	1800
	Compressive strength (f_{ck})	40	-
Mechanics	Flexural tensile strength (MPa)	3d: 0.84 / 7d: 2.28 / 28d: 4.0 / 63d: 4.4	-
	Modulus of elasticity (GPa)	3d: 14.6 / 7d: 24.1 / 28d: 30.0 / 63d: 32.0	0.002
	Thermal Expansion (10 ⁻⁶ /°C)	10	2
Viscoelastic	Coef. of creep [10 ⁻⁶ /MPa/ln(day)]	(a: 4.2 / b: 25.2) ⁽¹⁾	-
Thermal	Thermal conductivity (J/s/m°C)	2.5	0.694
	Specific heat (J/kg°C)	940	1000

Note: ⁽¹⁾Creep coefficient obtained through the expression of Botassi et al. [42] / (3d): at the age of 3 days / (7d): at the age of 7 days / (28d): at the age of 28 days / (63d): at the age of 63 days.

Figure 9 presents the proposed discretized model, for computational simulation in a transient regime.

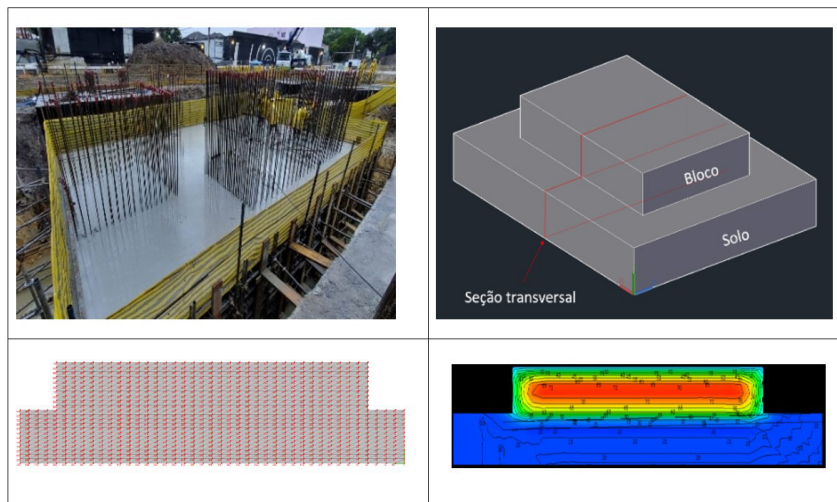


Figure 9. Discretized computational model for thermomechanical analysis of the proposed foundation block: (a) Photograph of the foundation block; (b) Volumetric representation (3d) of the materials considered in the thermomechanical simulation; (c) Square mesh of finite elements with maximum dimension of 25cm (cross section); (d) Development of temperatures along the cross-section.

Through Figures 10a and 10b, it is possible to observe the increase in the maximum internal temperatures (in the center of the block) for the pouring of concrete with a placing temperature of 30°C, as well as the maximum imposed and resistant stresses, respectively.

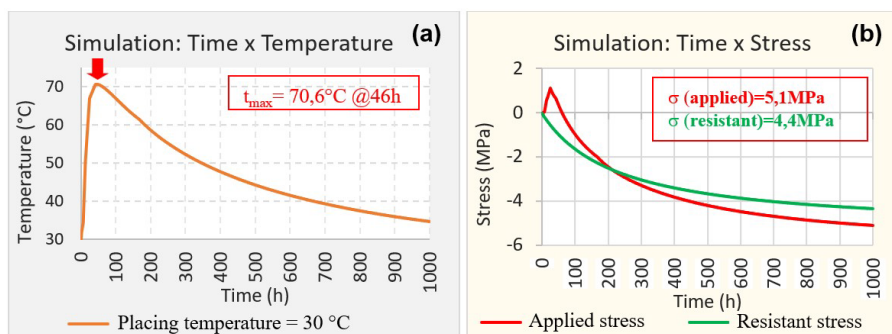


Figure 10. (a) Development of maximum internal temperatures at the center of the structural element – Placing temperature 30°C (simulation); (b) Development of the maximum applied and resistant stresses - Placing temperature 30°C (simulation).

It appears that the maximum internal temperature reached a peak of around 70.6°C within 46 hours after placing the concrete in the formwork (Figure 1a), indicating a high risk for the formation of DEF, as this value exceeds the critical range of 65°C to 70°C. The applied stresses exceeded the resistant ones approximately 220 hours into the simulation (Figure 10b), indicating a strong tendency for the concrete to crack.

Similarly, Figures 11a and 11b depict the development of maximum temperatures and internal stresses when placing concrete in the formwork at temperatures of 20°C (potentially cooled with the use of ice).

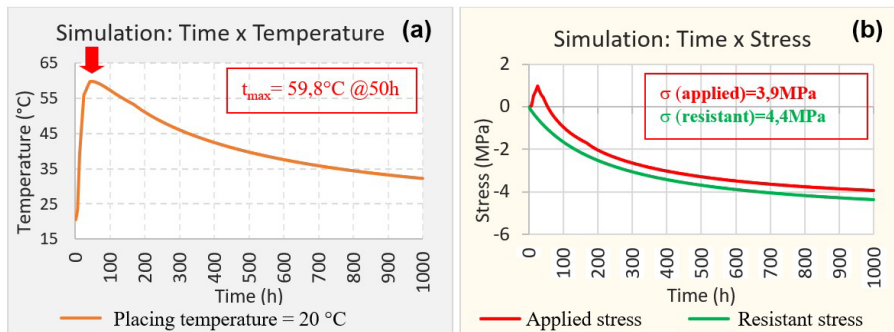


Figure 11. (a) Development of maximum internal temperatures at the center of the structural element – Placing temperature 20°C (simulation); (b) Development of the maximum applicand and resistant stresses - Placing temperature 20°C (simulation).

This time, the simulations indicate a maximum temperature peak of 59.8°C occurred after 50 hours of simulation, in the center of the structural element (Figure 11a), and the stresses did not exceed the tensile strength of the concrete at any moment, thermal cracking is less likely.

These results corroborate the responses obtained through the diagrams (Figures 7 and 8) which, expeditiously, enabled the preliminary assessment of thermo-tensional risk.

4.3 Validation: measured and simulated temperatures

Figure 12 shows the monitoring of the temperature rise of the concrete applied, measured at the geometric center of the foundation block. Monitoring was carried out for 118 hours and for this purpose a constantan copper “K” thermocouple cable was used, connected to a data logger by Extech, model SDL200.

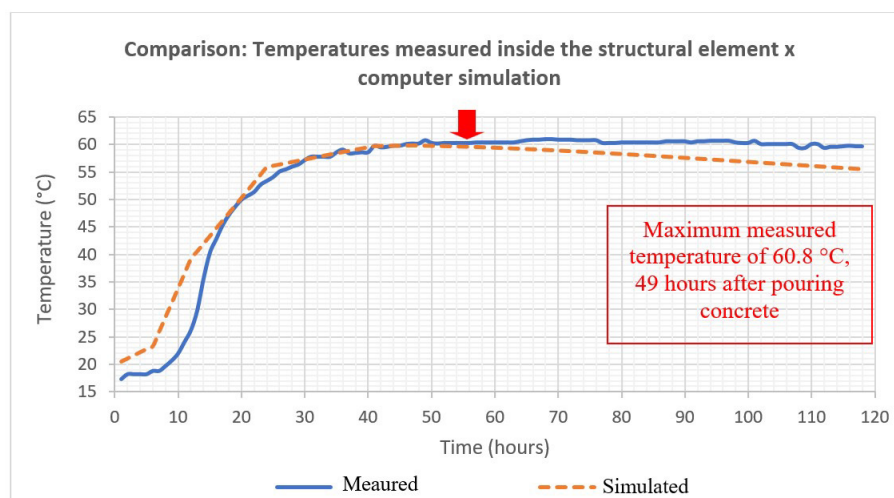


Figure 12. Concrete temperature evolution, measured using thermocouples in the geometric center of the foundation block x simulated.

The maximum temperature, which occurred in the center of the concrete element, reached a peak value of 60.8°C, after 49 hours of concreting. This value is very close to that obtained through simulation (59.8°C) expected to occur 50 hours after the start of concreting. The difference between predicted through simulation and what happened in practice was only 1.6%, revealing good adherence of the model to reality.

It is also important to note that due to the impossibility of effectively controlling variables such as the ambient temperature in a case study of this type, the actual average temperature of the concrete poured into the forms was 18°C, which is below the established critical limit of 20°C.

For comparison, in conditions where heat exchange is hindered (almost adiabatic condition), as in the core of large dimension elements, it is common to consider a proportional relationship between the placement temperature and the final maximum temperature reached. In other words, if the concrete were placed at 20°C, its maximum internal temperature would be approximately 62.8°C, incurring only a 5% deviation from what was predicted by the prior simulation and remaining below the 65°C mark.

Additionally, the software TSA-2D employs the thermochemical-mechanical approach for modeling and simulating structural elements. In this context, it is worth noting that this approach tends to yield results highly consistent with real measurements, as demonstrated in this and other previous studies [1]–[5].

5 CONCLUSIONS

It is considered that the expedited diagrams were satisfactory in the preliminary assessment of the thermal risk involved in pouring the proposed foundation block, making it possible to estimate it with good precision.

As already explained, the thermomechanical analysis of concrete is divided into two fundamental and indispensable parts: thermal and tensional. The thermal risk diagrams contemplate the thermal analysis of the concrete and indirectly address the effect associated with the tensional risk, which, as it involves parameters of greater complexity and is difficult to simplify, must have its analysis confirmed using computational models that faithfully represent field conditions.

Finally, although the thermal risk diagrams do not claim to assess the tensional risks involved, in cases where the response indicates 'low risk', and the limitations of the method were respected/considered, there were no indications of cracking due to thermal stresses in most of the analyzed models. Therefore, it is concluded that the expedited diagrams are a screening tool for structures that require additional care, preliminarily excluding those of 'low risk'. Furthermore, compared with computational thermal simulations, the method demonstrates good correlation, with potential application and reproducibility.

REFERENCES

- [1] C. Brites, R. Rocha, A. Vasconcellos, and P. Helene, "Estudo de caso envolvendo concretagens de elementos de fundação de grande porte: caso Parque da Cidade-SP," in *An. 55º Congr. Bras. Concr.*, Natal, 2014, pp. 1–13.
- [2] S. S. Botassi and F. L. Vieira, "Manifestação patológica precoce em bloco de fundação," *Concreto Construcoes*, vol. XLIX, no. 102, pp. 61–68, 2021, <http://doi.org/10.4322/1809-7197.2021.102.0003>.
- [3] D. Couto, P. Helene, and L. C. Almeida, "Temperature monitoring in large volume spread footing foundations: case study 'Parque da Cidade' - São Paulo," *Rev. IBRACON Estrut. Mater.*, vol. 9, no. 6, pp. 953–968, 2016, <http://doi.org/10.1590/s1983-41952016000600007>.
- [4] B. Pessoa, "Estudo térmico: diretrizes para a concretagem de bloco de fundação de edifício," Monography, Eng. Civil, Fac. Eng. São Paulo, São Paulo, 2019.
- [5] E. I. Funahashi Jr., S. C. Kuperman, and G. R. Vicente, "Simulação de tensões térmicas do bloco de fundação do edifício Paulista Corporate," in *An. 53º Congr. Bras. Concr.*, Florianópolis, 2011.
- [6] S. S. Botassi, *Fenômeno Térmico do Concreto: Análise Técnica e Simulações de Concretagem*, 1ª ed. Rio de Janeiro: Interciência, 2022, pp. 31–33.
- [7] A. M. Neville and J. J. Brooks, *Tecnologia do Concreto*, 2ª ed. Porto Alegre: Bookman, 2013.
- [8] P. K. Mehta and P. J. M. Monteiro, *Concreto: Microestrutura, Propriedades e Materiais*, 2ª ed. São Paulo: IBRACON, 2014.
- [9] American Concrete Institute, *Guide to Mass Concrete*, ACI 207.1R-05, 2005.
- [10] G. C. Isaia, Ed., *Concreto: Ciência e Tecnologia*, 1ª ed. São Paulo: IBRACON, 2011.
- [11] I. F. Torres and T. Andrade, "Risk analysis of the delayed ettringite formation in pile caps foundation in the metropolitan region of Recife – PE – Brasil," *Rev. IBRACON Estrut. Mater.*, vol. 9, no. 3, pp. 357–394, 2016, <http://doi.org/10.1590/S1983-41952016000300003>.
- [12] M. Collepardi, "A state-of-the art review on delayed ettringite attack on concrete," *Cement Concr. Compos.*, vol. 25, no. 4-5, pp. 401–407, 2003., [http://doi.org/10.1016/S0958-9465\(02\)00080-X](http://doi.org/10.1016/S0958-9465(02)00080-X).

- [13] S. K. Melo, "Estudo da formação da etringita tardia em concreto por calor de hidratação do cimento," M.S. thesis, Univ. Fed. Goiás, Goiânia, 2010.
- [14] N. Hasparik et al., "Ataque combinado da RAA e DEF em concreto de fundação de edificação," *Conc. Constr.*, no. 74, pp. 100–108, 2014.
- [15] Pesavento et al., "Numerical modelling," in *Thermal Cracking of Massive Concrete Structures – State of the Art Report of the RILEM Technical Committee 254-CMS* (Vol. 27), E. M. R. Fairbairn and M. Azenha, Eds., Switzerland, 2019, ch. 7, pp. 181–225.
- [16] D. Gawin, F. Pesavento, and B. A. Schrefler, "Hygro-thermo-chemo-mechanical modelling of concrete at early ages and beyond. Part I: Hydration and hygro-thermal phenomena," *Int. J. Numer. Methods Eng.*, vol. 67, no. 3, pp. 299–331, 2006., <http://doi.org/10.1002/nme.1615>.
- [17] A. Loukili, D. Chopin, A. Khelidj, and J. Y. Le Touzo, "A new approach to determine autogenous shrinkage of mortar at an early age considering temperature history," *Cement Concr. Res.*, vol. 30, no. 6, pp. 915–922, 2000, [http://doi.org/10.1016/S0008-8846\(00\)00241-6](http://doi.org/10.1016/S0008-8846(00)00241-6).
- [18] E. M. R. Fairbairn, M. M. Silvano, R. D. Toledo Fo., J. L. D. Alves, and N. F. F. Ebecken, "Optimization of mass concrete construction using genetic algorithms," *Comput. Struct.*, vol. 82, no. 2-3, pp. 281–299, 2004, <http://doi.org/10.1016/j.compstruc.2003.08.008>.
- [19] R. Faria, M. Azenha, and J. A. Figueiras, "Modelling of concrete at early ages: application to an externally restrained slab," *Cement Concr. Compos.*, vol. 28, no. 6, pp. 572–585, 2006, <http://doi.org/10.1016/j.cemconcomp.2006.02.012>.
- [20] T. Honorio, B. Bary, and F. Benboudjema, "Evaluation of the contribution of boundary and initial conditions in the chemo-thermal analysis of a massive concrete structure," *Eng. Struct.*, vol. 80, pp. 173–188, 2014, <http://doi.org/10.1016/j.engstruct.2014.08.050>.
- [21] F.-J. Ulm and O. Coussy, "What is a "massive" concrete structure at early ages? Some dimensional arguments," *J. Eng. Mech.*, vol. 127, no. 5, pp. 512–522, 2001, [http://doi.org/10.1061/\(ASCE\)0733-9399\(2001\)127:5\(512\)](http://doi.org/10.1061/(ASCE)0733-9399(2001)127:5(512)).
- [22] S. S. Botassi, *Fenômeno Térmico do Concreto: Fundamentos e Aplicações Práticas*, 1ª ed. Rio de Janeiro: Interciência, 2019.
- [23] American Concrete Institute, *Specification for Structural Concrete*, ACI 301-10, 2010.
- [24] G. R. Vicente, S. Kuperman, and E. I. Funahashi Jr., "Fissuração de origem térmica em blocos de fundação: Quando refrigerar o concreto?," in *An. 56º Congr. Bras. Concr.*, 2014.
- [25] A. A. Demétrio Fo., J. R. Carvalho, R. A. P. Moraes, and T. W. C. O. Andrade, *Cuidados na Execução de Fundações em Concreto-Massa: Edificações Verticais*, 1ª ed. Recife, Tecomat Eng., 2020.
- [26] C. P. Bobko, *Crack Free Mass Concrete Footings on Bridges in Coastal Environments*. Raleigh: Dept. Civ. Constr. Environ. Eng. North Carolina State Univ., 2014.
- [27] American Concrete Institute, *Report on Thermal and Volume Change Effects on Cracking of Mass Concrete*, ACI 207.2R-07, 2007.
- [28] Associação Brasileira de Normas Técnicas, *Cimento Portland – Requisitos*, ABNT NBR 16697, 2018.
- [29] K. Flaga "Macro self-induced thermal stresses in concrete elements and structures". Monograph 106. Cracow Technical University, 1990.
- [30] F. Kanavaris et al., "Enhanced massivity index based on evidence from case studies: Towards a robust pre-design assessment of early-age thermal cracking risk and practical recommendations," *Constr. Build. Mater.*, vol. 271, pp. 121570–121587, 2021, <http://doi.org/10.1016/j.conbuildmat.2020.121570>.
- [31] American Society for Testing and Materials, *Standard Specification for Portland Cement*, ASTM C150/C150M, 2022.
- [32] J. Gajda, "When should mass concrete requirements apply?," *Aspire Magazine*, 2015.
- [33] Editora Interciência-on. "TSA-2D." SBS Consultoria em Engenharia, 2021. <https://www.editorainterciencia.com.br/downloads/programas/Executaveis.zip> (accessed Sept. 7, 2023).
- [34] Associação Brasileira de Normas Técnicas, *Cimento – Determinação do Calor de Hidratação pelo Método de Garrafa de Langavant – Método de Ensaio*, ABNT NBR 12006, 1990.
- [35] S. S. Botassi, "Uma contribuição ao estudo do comportamento termomecânico de estruturas maciças de concreto: modelagem viscoelástica linear e aplicações," M.S. thesis, Univ. Fed. Espírito Santo, Vitória, 2004.
- [36] M. Emborg, "Thermal stresses in concrete structures at early ages," Ph.D. dissertation, Lulea Univ. Technol., Lulea, Swedish, 1989.
- [37] F. Kreith and W. Z. Black, *La Transmision del Calor*. Madrid: Alhambra S.A, 1983.
- [38] E. I. Funahashi Jr, S. C. Kuperman, G. R. Vicente, F. Sobrinho, and R. Valtorta, "Práticas recomendadas para execução do bloco de fundação do edifício grande Ufficiale Evaristo Comolatti," in *An. 60º Congr. Bras. Concr.*, 2018.
- [39] E. A. Gamballe, A. Castro, M. A. S. Andrade, and M. Traboulsi, "Análise estatística dos parâmetros que intervêm no fenômeno térmico do concreto massa," in *An. 52º Congr. Bras. Concr.*, 2010.
- [40] Associação Brasileira de Normas Técnicas, *Projeto de Estruturas de Concreto – Procedimento*, ABNT NBR 6118, 2014.
- [41] U. S. Bureau of Reclamation, *Creep of Concrete Under High Intensity Loading* (Concrete Laboratory Report C-820). Denver, 1956.

- [42] S. S. Botassi et al., “Modelo de predição da fluência com base em banco de dados do laboratório de concreto de furnas: estudos preliminares,” in *An. 49º Congr. Bras. Concr.*, 2007.
- [43] V. A. Paulon, *O Fenômeno Térmico do Concreto* (Estudo Técnico 85, pp. 1–42). ABCP, 1987.

Author contributions: BP: conceptualization, data curation, formal analysis, methodology, software, writing; CB: formal analysis, methodology, supervision, writing; SB: formal analysis (supporting), writing (review and editing); JD: formal analysis (supporting), writing (review and editing); MC: formal analysis (supporting), writing (review and editing); DC: formal analysis (supporting), writing (review and editing); CMG: formal analysis (supporting), writing (review and editing).

Editors: Fernando Pelisser, Daniel Carlos Taissum Cardoso.